Biochimica et Biophysica Acta 1850 (2015) 43–50

Contents lists available at ScienceDirect

Biochimica et Biophysica Acta

journal homepage: www.elsevier.com/locate/bbagen

A novel ATP-generating machinery to counter nitrosative stress is mediated by substrate-level phosphorylation

Christopher Auger, Vasu D. Appanna *

Faculty of Science & Engineering, Laurentian University, Sudbury, Ontario P3E 2C6, Canada

ARTICLE INFO

Article history:
Received 2 July 2014
Received in revised form 19 September 2014
Accepted 30 September 2014
Available online 7 October 2014

Keywords:
Metabolon
Reactive nitrogen species
Phosphotransfer
Metabolism
Microbiology

ABSTRACT

Background: It is well-known that elevated amounts of nitric oxide and other reactive nitrogen species (RNS) impact negatively on the tricarboxylic acid (TCA) cycle and oxidative phosphorylation. These perturbations severely compromise O_2-dependent energy production. While bacteria are known to adapt to RNS, a key tool employed by macrophages to combat infections, the exact mechanisms are unknown.
Methods: The bacterium was cultured in a defined mineral medium and cell-free extracts obtained at the same growth phase were utilized for various biochemical studies Blue native polyacrylamide gel electrophoresis followed by in-gel activity assays, high performance liquid chromatography and co-immunoprecipitaton are applied to investigate the effects of RNS on the model microbe *Pseudomonas fluorescens*.
Results: Citrate is channeled away from the tricarboxylic acid cycle using a novel metabolon consisting of citrate lyase (CL), phosphoenolpyruvate carboxylase (PEPC) and pyruvate phosphate dikinase (PPDK). This metabolic engine comprising three disparate enzymes appears to transiently assemble as a supercomplex aimed at ATP synthesis. The up-regulation in the activities of adenylate kinase (AK) and nucleoside diphosphate kinase (NDPK) ensured the efficacy of this ATP-making machine.
Conclusion: Microbes may escape the effects of nitrosative stress by re-engineering metabolic networks in order to generate and store ATP anaerobically when the electron transport chain is defective.
General significance: The molecular configuration described herein provides further understanding of how metabolism plays a key role in the adaptation to nitrosative stress and reveals novel targets that will inform the development of antimicrobial agents to counter RNS-resistant pathogens.

1. Introduction

ATP is the universal energy currency in all living organisms and its adequate supply is central to the survival and propagation of life. This adenine moiety is commonly generated via substrate-level phosphorylation (SLP), photophosphorylation and oxidative phosphorylation. In aerobes, ATP stems predominantly from the latter [1]. The NADH and $FADH_2$ formed via the tricarboxylic acid (TCA) cycle provide the reductive potential necessary to synthesize the high-energy phosphate. If not immediately required to accomplish cellular work, this moiety can be distributed throughout the cell in the form of high-energy compounds such as phosphocreatine, acetyl-phosphate, polyphosphates, phosphorylated nucleosides and/or stored as energy reserves in the form of carbohydrates and fatty acids [2,3].

In an effort to maximize the production of ATP during oxidative phosphorylation, an intimate interaction between complex V, the ATP-synthesizing machine and various kinases does exist [4,5]. This allows for the rapid transfer of phosphate from ATP with the concomitant formation of a high-energy compound and ADP. Indeed, such a system further drives the ATP-making process. These phosphotransfer networks are crucial to the bioenergetics of an organism, ensuring an intricate balance between ATP-generating and consuming processes. In the absence of operative machinery mediated by the electron transport chain (ETC), the generation of ATP must proceed through SLP. In this instance, cellular metabolism gives rise to energy-rich phosphorylated compounds that are tapped as ATP [6]. Phosphoenolpyruvate (PEP) and 1,3-biphosphoglycerate are two key glycolytic intermediates that enable anaerobic organisms to fulfill their energy needs [7,8].

Due to their reliance on redox metals, the complexes of the ETC present themselves as ideal targets for free radicals within the cell [9,10]. Nitric oxide (NO) stress is known to severely hinder oxidative phosphorylation and hence the ability of organisms to derive their ATP needs via this machinery [11]. Therefore, if an organism subjected to these insults is to survive, it must devise alternative ATP-producing

Abbreviations: ACK, acetate kinase; ADP, adenosine diphosphate; AK, adenylate kinase; AMP, adenosine monophosphate; ATP, adenosine triphosphate; BN-PAGE, blue native polyacrylamide gel electrophoresis; CFE, cell-free extract; CL, citrate lyase; DEANO, diethylamine NONOate; ETC, electron transport chain; G6PDH, glucose-6-phosphate dehydrogenase; HPLC, high performance liquid chromatography; NDPK, nucleoside diphosphate kinase; NO, nitric oxide; PEP, phosphoenolpyruvate; PEPC, phosphoenolpyruvate carboxylase; PK, pyruvate kinase; PPDK, pyruvate, phosphate dikinase; RNS, reactive nitrogen species; SLP, substrate-level phosphorylation; SNP, sodium nitroprusside; TCA, tricarboxylic acid

* Corresponding author. Tel.: +1 705 675 1151x2112; fax: +1 705 675 4844.
E-mail address: vappanna@laurentian.ca (V.D. Appanna).

http://dx.doi.org/10.1016/j.bbagen.2014.09.028
0304-4165/

strategies. Although a body of literature on the detoxification of NO and reactive nitrogen species (RNS) exists, the molecular details on how organisms fulfill their ATP requirements during this challenge have yet to be unraveled [12–14]. In this study we have examined the ability of *Pseudomonas fluorescens*, a model microbe with genetic traits similar to the opportunistic pathogen *Pseudomonas aeruginosa*, to generate ATP in response to RNS-induced defective oxidative phosphorylation [15]. The assembly of an ATP-generating supercomplex, in addition to the increased activity of enzymes mediating the transfer of high-energy phosphate, allows the microbe to survive and proliferate despite the onslaught of RNS. The significance of metabolic networks and phosphotransfer systems in maintaining ATP homeostasis is discussed. The targeting of these enzymes in RNS-resistance microbes is also commented on.

2. Materials and methods

2.1. Cell culturing and fractionation

P. fluorescens 13525, obtained from the American Type Culture Collection (ATCC), was cultured on 2% agar and grown in a phosphate mineral medium containing Na_2HPO_4 (6 g), KH_2PO_4 (3 g), $MgSO_4 \cdot 7H_2O$ (0.2 g), NH_4Cl (0.8 g), and citric acid (4 g) per litre of distilled and deionized H_2O (ddH_2O). Trace elements were added to a final concentration of 1%, as described previously, and NaOH was utilized to adjust the pH to 6.8 prior to autoclaving at 121 °C for 20 min [16,17]. One milliliter of *P. fluorescens* grown to stationary phase in a control culture was introduced to 200 mL of media in an Erlenmeyer flask. To the media, sodium nitroprusside (SNP, 10 mM) or diethylamine NONOate (DEANO; 0.5, 1 mM) was added. DEANO and SNP are both initiators of nitrosative stress via the release of NO [18,19]. A second dose of DEANO was added during the exponential growth phase (16 h) to maintain NO levels in the medium. Cultures treated with SNP were grown alongside cultures with 10 mM sodium ferrocyanide as a control. The latter has a similar structure to SNP minus the nitroso functional group [20]. As DEANO and SNP are both initiators of nitrosative stress and generated similar physiological results, they were used interchangeably. Bacteria were grown and aerated on a gyratory water bath shaker (Model 76; New Brunswick Scientific). After 24 h of growth, cells reached their stationary phase and were isolated by centrifugation (10, 000 ×*g*, 10 min, 4 °C). Pellets were washed with 0.85% NaCl and re-suspended in cell storage buffer (CSB; 50 mM Tris–HCl, 5 mM $MgCl_2$, 1 mM phenylmethylsulphonyl fluoride, pH 7.3).

Cell pellets were disrupted ultrasonically and then centrifuged at 3000 ×*g* for 30 min at 4 °C to remove intact bacteria. Soluble and membrane cell-free extracts (CFE) were then obtained by centrifugation at 180,000 ×*g* for 3 h. Purity of the fractions was assessed via the analysis of glucose-6-phosphate dehydrogenase (G6PDH) and complex IV activity in the soluble and membrane portions, respectively. Protein quantities were ascertained in triplicate with bovine serum albumin as a standard, using the Bradford assay [21]. CFE fractions were prepared immediately for in-gel activity assays and frozen at −20 °C for storage up to a maximum of 4 weeks.

2.2. Blue native polyacrylamide gel electrophoresis (BN-PAGE) in-gel activity assays

BN-PAGE and activity assays were performed as described [22,23]. To ensure optimal protein separation, 4–16% linear gradient gels were cast with the Bio-Rad MiniProtean™ 2 system using 1 mm spacers. Soluble CFE was prepared in a native buffer (50 mM Bis–Tris, 500 mM ε-aminocaproic acid, pH 7.0, 4 °C) at a final concentration of 4 mg of

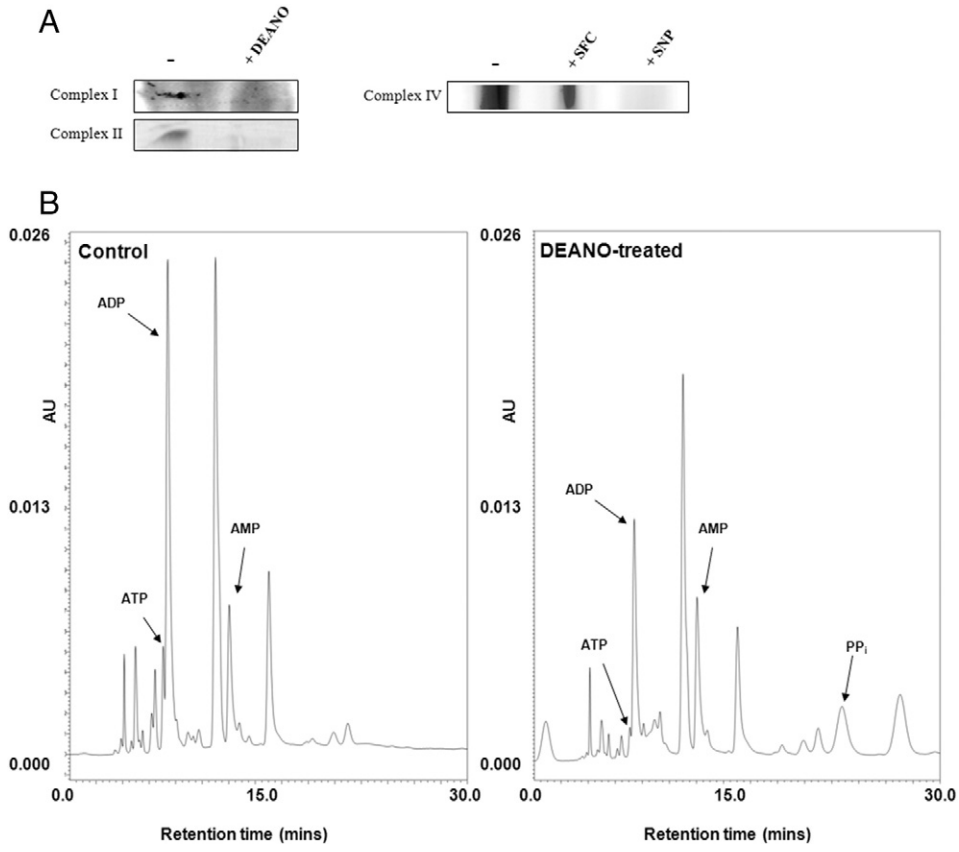

Fig. 1. Nucleotide and ETC analysis in *P. fluorescens* exposed to nitrosative stress. A; In-gel activity assays of protein complexes from the electron transport chain (–, untreated; + DEANO, 1 mM diethylamine NONOate, + SFC, 10 mM sodium ferrocyanide; + SNP, 10 mM sodium nitroprusside). Images shown are representative gels; $n = 3$. B; Representative chromatographs displaying nucleotide levels in soluble cell free extract from *P. fluorescens* grown in control cultures and 1 mM DEANO-containing cultures; $n = 3$.

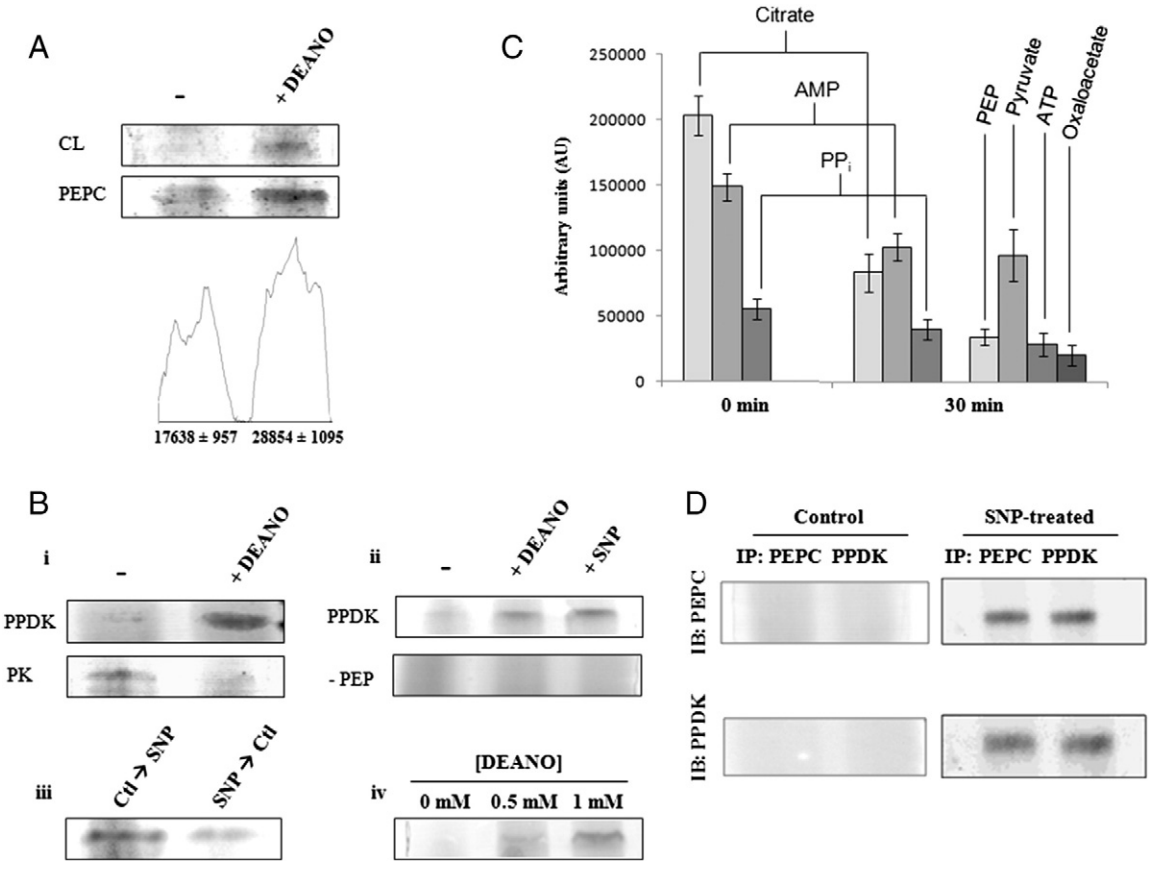

Fig. 2. ATP-producing supercomplex. A; Enzymes participating in the metabolism of citrate were probed by BN-PAGE in control (−) and 1 mM DEANO-treated cultures (CL, citrate lyase; PEPC, phosphoenolpyruvate carboxylase). B; i) the activity of phosphoenolpyruvate-dependent kinases was analyzed in-gel. ii) Reaction mixture without phosphoenolpyruvate served as a negative control. iii) PPDK activity subsequent to regulation experiments. Control cells were incubated in 10 mM SNP-containing medium for 8 h and vice versa prior to activity assays. iv) PPDK dose response with DEANO. C; The activity band for CL was excised from the gel and incubated in reaction buffer containing 2 mM citrate, 0.5 mM AMP and 0.5 mM PP_i. Consumption of the substrates and appearance of products was monitored by HPLC. n = 3 ± standard deviation. D; Soluble CFE from control and SNP-treated cultures were utilized for immunoprecipitation (IP) using antibodies against PEPC or PPDK. The immunoprecipitates were separated on 10% SDS-PAGE, transferred and an immunoblot (IB) was performed to analyze bound proteins (PEPC, phosphoenolpyruvate carboxylase; PK, pyruvate kinase; PPDK, pyruvate phosphate dikinase) Images shown are representative gels; $n = 3$. ImageJ for Windows was used to perform densitometry.

protein per mL. Membrane CFE was prepared in a similar manner except β-dodecyl-D-maltoside was added at a concentration of 1% to the preparation to facilitate the solubilization of membrane-bound proteins. Equal protein loading was ensured by monitoring protein concentration using the Bradford assay. Each well was loaded with 60 μg of protein prior to electrophoresis. The latter was performed at 4 °C under native conditions at 80 V and 15 mA for proper stacking, followed by 150 V and 25 mA until the migration of the proteins reached half way through the resolving gel. At the halfway point, blue cathode buffer (50 mM Tricine, 15 mM Bis–Tris, 0.02% *w/v* Coomassie G-250, pH 7 at 4 °C) was changed to a colorless cathode buffer (50 mM Tricine, 15 mM Bis–Tris, pH 7 at 4 °C). The electrophoresis was performed at 300 V and 25 mA beyond this point. Following electrophoresis, gel slabs were equilibrated for 15 min in a reaction buffer (25 mM Tris–HCl, 5 mM $MgCl_2$, at pH 7.4). Afterwards, enzyme activities were detected using select reaction mixtures.

The functionality of ETC complexes was ascertained as described [9,24]. CL and PEPC reaction mixtures were prepared, containing citrate and PEP as reactions substrates respectively, as demonstrated in [11]. PK and PPDK activity assays were performed as shown [25]. The activity of NDPK was probed using the enzymes hexokinase and G6PDH as elaborated in [26]. Acetate kinase (ACK) was analyzed in-gel with a reaction mixture consisting of 5 mM acetyl-phosphate, 1 mM ADP, 5 mM glucose, 10 units of G6PDH, 10 units of hexokinase, 1 mM NADP, 0.2 mg/mL of phenazine methosulfate (PMS) and 0.4 mg/mL of iodonitrotetrazolium (INT). ATP formation allows the synthesis of glucose-6-phosphate, which is coupled to G6PDH activity, allowing NADP reduction and formazan precipitation at the site of the enzyme *in situ*. Negative controls were performed without acetyl-phsophate or without glucose. Adenylate kinase activity was discerned with a reaction mixture containing 10 mM ADP, 5 mM glucose, 0.5 mM NADP, 10 units of hexokinase, 10 units of G6PDH, 0.2 mg/mL of PMS and 0.4 mg/mL of INT. Negative controls consisted of the same reaction mixture without ADP or without glucose. PPase activity was monitored in-gel via the formation of a phosphomolybdate complex with malachite green, as described [27]. Destaining solution (40% methanol and 10% glacial acetic acid) was used to terminate the reactions. Coomassie blue staining was applied to assure equal protein loading. To identify optimal conditions for these reactions, substrate concentrations and incubation times were varied. Select activity bands were submitted to densitometry using ImageJ for Windows. All comparative experiments were performed at the late logarithmic phase of growth. BSA (66 kDa) and ferritin (450 kDa) were used as molecular weight standards in a separate lane of the BN-PAGE gel.

2.3. Enzyme confirmation and metabolite analyses via HPLC

To evaluate the influence of nitrosative stress on metabolite levels, these were analyzed by high performance liquid chromatography (HPLC). Metabolites were separated using a C_{18} column with a polar cap (3.5 μm, amide cap, 4.6 mm × 150 mm inside diameter, Symmetry Column, Phenomenex®, Torrance, CA, USA). The mobile phase

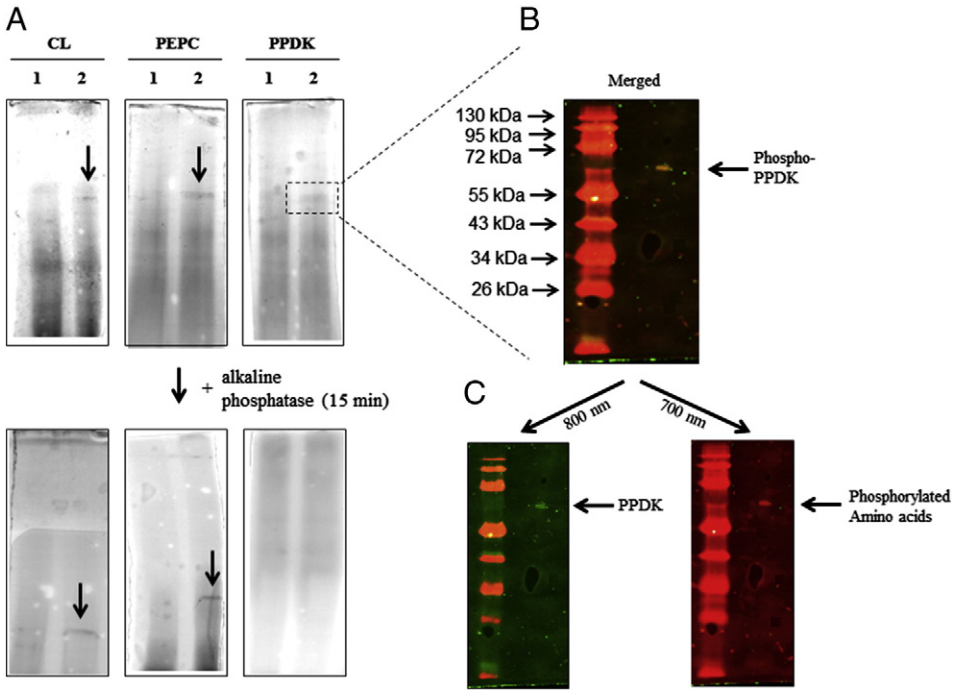

Fig. 3. Phosphorylation and dissociation of ATP-generating machinery. A; CL, PEPC and PPDK were probed with their respective reaction mixtures and activity bands were identified at a similar spot in the gel (top). Soluble CFE treated with 20 U of alkaline phosphatase for 15 min prior to BN-PAGE was loaded into wells and activity assays were performed after electrophoresis. CL and PEPC appeared lower in the gel after treatment, while PPDK activity was notably absent (1, Control; 2, 10 mM SNP-treated). B; the band attributed to PPDK was excised and loaded into a 10% SDS gel. Following electrophoresis and protein transfer, the membrane was submitted to Western blot analysis. Anti-PPDK antibodies (green—800 nm) and antibodies versus phosphoserine/threonine/tyrosine (red—680 nm) were applied and a yellow band was generated using IR-tagged secondary antibodies. C; A band at 60 kDa, the reported molecular weight of PPDK, was visible in both channels. Images shown are representative gels; $n = 4$.

consisted of 20 mM KH_2PO_4 (pH 2.9 with 6 N HCl) prepared in Milli-Q water and the column was eluted at a flow rate of 0.7 mL/min at 25 °C. A 2 mg protein equivalent of soluble CFE from control and 1 mM DEANO-treated cells was boiled for 5 min to precipitate protein prior to injection. Nucleotides were detected at 254 nm, while organic acids were visualized at 210 nm using a Waters UV–visible detector. Metabolites were identified by spiking biological samples with known standards, and peaks were quantified using the Empower software (Waters Corporation). The HPLC was standardized using a five-point calibration prior to each injection protocol.

The BN-PAGE activity band belonging to CL/PEPC/PPDK was rinsed twice with reaction buffer, excised from the gel and placed in reaction buffer containing 2 mM citrate, 0.5 mM AMP and 0.5 mM PP_i. After 30 min of incubation, 100 μL of the sample was collected and diluted ten-fold with Milli-Q water for HPLC analysis. While multiple time points were taken, a 30 min incubation afforded optimal results. Samples were injected immediately after the reactions in order to minimize substrate and product degradation. A similar protocol was applied to ascertain the nature of the activity band for AK. However, the reaction buffer solely contained 0.5 mM ADP, and was allowed to react with the enzyme for 45 min prior to injection.

2.4. 2D SDS-PAGE and Western blots

The activity band for CL/PEPC/PPDK was precision cut from the gel and incubated at ambient temperature for 30 min in a denaturing solution of 1% (*w*/*v*) SDS and 1% (*v*/*v*) 2-mercaptoethanol. The band was rinsed twice for 10 s with SDS-PAGE electrophoresis buffer (25 mM Tris–HCl, 192 mM glycine and 0.1% (*w*/*v*) SDS; pH 8.3) then placed vertically in the well of a 10% isocratic SDS gel (8 × 7 cm). SDS-PAGE was performed according to a modified protocol [28]. Electrophoresis was conducted at 80 V at room temperature until the proteins reached the separating gel. The voltage was then raised to 200 V until completion. The molecular mass of proteins was assessed using the EZ-Run Prestained Recombinant Protein Ladder (Fisher Scientific). Following electrophoresis, the proteins were transferred for 16 h at 25 V on to a nitrocellulose membrane (Li-COR) for Western blots. Non-specific binding sites on the membrane were blocked by treatment with 5% non-fat skim milk dissolved in TTBS [20 mM Tris–HCl, 0.8% NaCl, 1% Tween-20 (pH7.6)] for 1 h. Primary antibodies directed toward PEPC (Rabbit polyclonal; dilution: 1:500; Abcam), PPDK (Rabbit polyclonal; dilution: 1:1000; generous gift from Dr. Frédéric Bringaud [Université Bordeaux Segalen, France]) and phosphoserine/threonine/tyrosine (Mouse monoclonal; dilution: 1:200, Abcam) were diluted in TTBS and incubated with the membrane for 1 h. The secondary antibodies consisted of donkey anti-rabbit infrared (IR) 800-conjugated (LI-COR) and donkey anti-mouse IR 680-conjugated (LI-COR) and were applied for 1 h in the dark in TTBS. Protein expression was documented using an Odyssey Infrared Imager and accompanying software (LI-COR. Lincoln, NE, USA) which detected an infrared signal from the conjugated secondary antibody at $\lambda_{excitation} = 778$ nm, $\lambda_{emission} = 795$ nm (IR 800) or $\lambda_{excitation} = 676$ nm, $\lambda_{emission} = 693$ nm (IR 680).

2.5. Supercomplex analyses and dissociation

BN-PAGE in-gel assays for CL, PEPC and PPDK revealed an activity band at a similar spot for all three enzymes, despite their disparate molecular masses. Incubation of this activity band in a solution of citrate, AMP and PP_i, as described above, did indeed generate pyruvate and ATP. This intriguing finding prompted us to explore whether any post-translational modifications may be involved in the formation of this metabolon. As such, bands were excised and loaded into a SDS gel for immunoblot analyses. Antibodies versus acetylated lysine residues (Rabbit polyclonal; dilution: 1:500; Abcam) and nitrosylated tyrosines (Mouse monoclonal; dilution: 1:1400; Abcam) did not generate a signal. In an attempt to dissociate these three enzymes, soluble CFE (at 4 mg protein/mL) was incubated with alkaline phosphatase (20 U) for 15 min at room temperature before BN-PAGE. Indeed, this proved

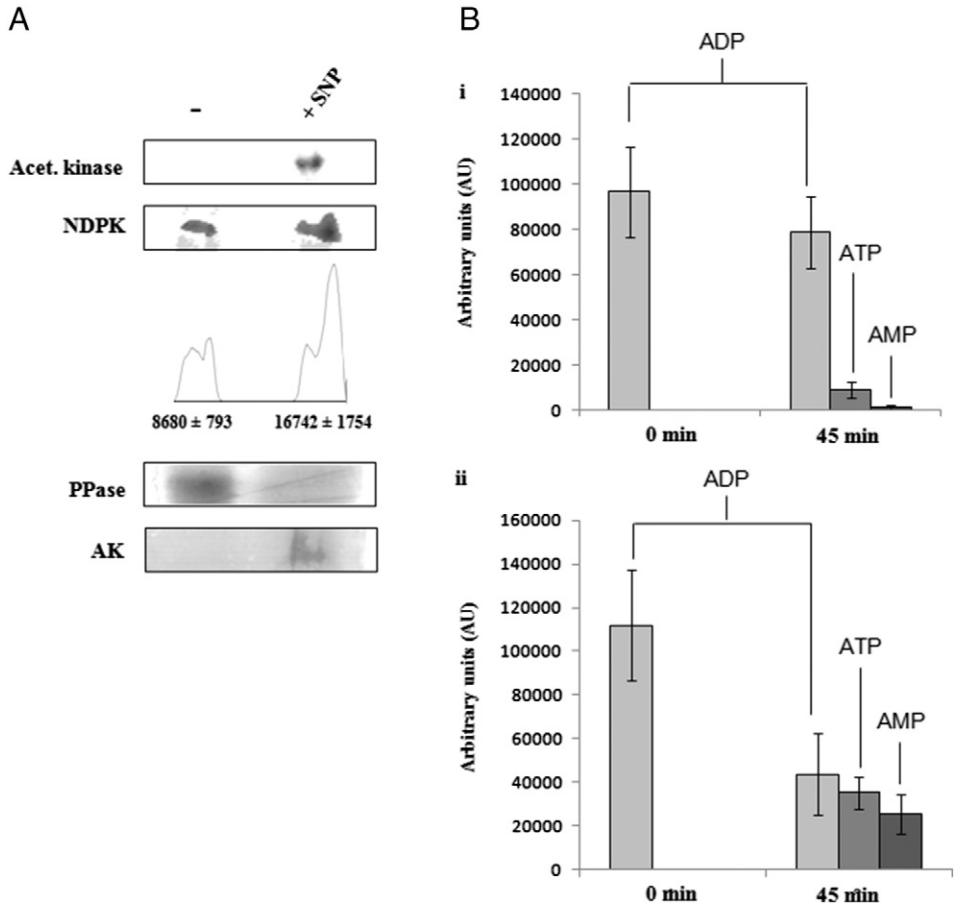

Fig. 4. Nucleotide production and phosphotransfer networks. A; The activity of various phosphotransfer enzymes was monitored in-gel. ImageJ for Windows was used to perform densitometry (AK, adenylate kinase; NDPK, nucleoside diphosphate kinase; PPase, inorganic pyrophosphatase). Gels are representative; $n = 3$. B; The activity band for AK from control (i) and 10 mM SNP-treated (ii) cells was excised and incubated in a solution of 0.5 mM ADP for 45 min. The appearance of products was monitored by HPLC; $n = 3 \pm$ standard deviation.

effective, indicating that a phosphorylation event was involved in metabolon formation. The link between proteins was further explored via pull-down assays.

2.6. Co-immunoprecipitation

Pull-down experiments were performed according to the manufacturer's instructions (Abcam). Cell pellets were lysed in 100 μL lysis buffer (1% maltoside, 1 mg/mL BSA, pepstatin A, leupeptin) for 60 min on ice with occasional vortexing. Agarose anti-IgG conjugates were prepared by diluting them 1:1 in dilution buffer (1% maltoside, 1 mg/mL BSA). Ten microliters of agarose conjugates was added to lysed samples and left to incubate for 1 h at 4 °C with gentle shaking to remove proteins which spontaneously bind to the agarose anti IgG conjugates. Samples were centrifuged at 200 *g* for 1 min and the supernatant was saved. Ten microliters of polyclonal anti-PPDK or 20 μL of polyclonal anti-PEPC was added to the diluted lysate for 1 h at 4 °C with gentle shaking. Following incubation with the primary antibody, 50 μL of agarose IgG conjugate was added per tube and allowed to incubate for 1 h with gentle shaking at 4 °C. Following incubation, samples were centrifuged at 200 *g* for 5 s. The supernatant was removed and the pellet was re-suspended in 500 μL of dilution buffer then centrifuged again at 200 g for 5 s. The supernatant was removed and the pellet was re-suspended in TBS and centrifuged. Re-suspension and centrifugation were repeated one more time using a solution of 0.5 M Tris at a pH of 6.8. The pellet was re-suspended in SDS-PAGE sample buffer and heated for 5 min at 100 °C. The sample was centrifuged at 200 *g* for 5 s and the supernatant was loaded onto a 10% SDS gel. A Western blot was performed on PEPC or PPDK, as described above.

2.7. Recovery experiments and statistical analysis

The NO-mediated modulation of PPDK activity was further confirmed with regulation experiments. Control cells grown in citrate medium for 24 h were transferred to a 10 mM SNP-containing medium. Following an 8 h exposure, the cells were collected and processed for BN PAGE as described above. Similar experiments were performed with 10 mM SNP-stressed cells transferred into a control medium. Data were expressed as means ± standard deviations. All experiments were performed in triplicate and biological duplicate.

3. Results

P. fluorescens was grown in a citrate medium with or without a NO donor until the culture reached its stationary phase, as measured by Bradford assay. At this point, bacteria were spun out of solution by centrifugation and the pellets submitted to sonication to separate the soluble and membrane fractions. The latter was prepared for BN-PAGE in order to ascertain the effect of NO on the ETC. Indeed, the addition of SNP or DEANO to the growth medium severely impeded complex I, II and IV, as visualized by in-gel activity assays (Fig. 1A). Given the repercussions of a defective ETC, the cytoplasm was subjected to HPLC analysis with a UV–visible detector set to 254 nm to identify nucleotides. While ADP and ATP levels in the RNS-treated cells were diminished, there was a slight increase in AMP and a large increase in pyrophosphate, as seen in chromatograms (Fig. 1B; ATP values determined by the area under the curve were 42 565 ± 3678 AU for the control and 14 326 ± 2479 AU for the nitrosative stress samples, respectively).

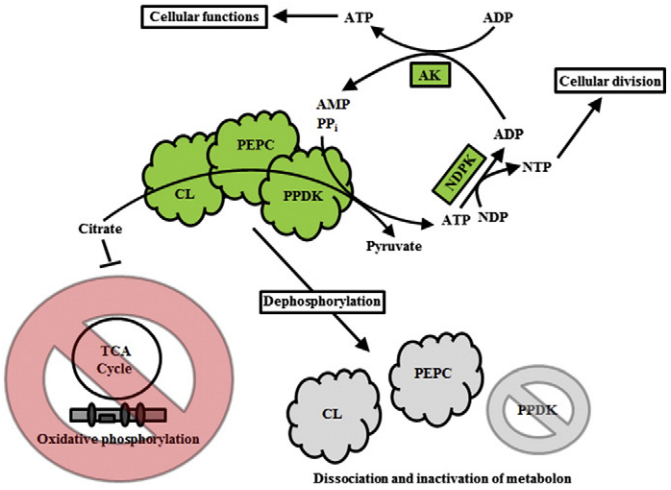

Fig. 5. Bioenergetics in *Pseudomonas fluorescens* exposed to nitrosative stress. A supercomplex involving CL, PEPC and PPDK is assembled by the organism to effectively produce ATP, while phosphotransfer networks permit the storage of this crucial moiety (red: enzymes inactivated by nitrosative stress; green: enzymes up-regulated during nitrosative stress; gray = metabolon enzymes disassociated by dephosphorylation).

These data suggest that nitrosative stress triggers a shift in the bioenergetics of the organism.

We have previously shown that, to counteract the detrimental effects of RNS on oxidative phosphorylation, the microbe up-regulates the activity and expression of CL in order to bypass the TCA cycle and generate energy in an anaerobic manner [11]. Here, it can be seen that CL and PEPC activities are sharply increased in order to generate the high-energy compound PEP when the microbe undergoes treatment with DEANO (Fig. 2A). PK, the usual candidate for the production of pyruvate and ATP, was noticeably inactive in the stress, whereas PPDK was up-regulated in the DEANO-treated cultures (Fig. 2B, i). This shift was apparent with the NO donor SNP as well. Reaction substrates, such as PEP, were routinely omitted from the in-gel activity assays to serve as a negative control. (Fig. 2B, ii). To confirm that NO donors were indeed triggering the metabolic reconfiguration, regulation experiments were performed. Cells cultured to the stationary phase with SNP were transferred to control medium for 8 h and vice versa. As shown, PPDK activity was lowered as the cells returned to an untreated environment (Fig. 2B, iii).

The primary advantage of the BN-PAGE system is that proteins remain in their native state, allowing the study of their interactions with other biomolecules as they would occur *in vivo* [29,30]. The lowered activity of aconitase, a consequence of intracellular RNS, causes an up-regulation of CL, PEPC, and PPDK. Despite these three enzymes having different molecular masses, the formazan precipitate indicative of enzymatic activity appeared at the same location in the gel, perhaps indicating that CL, PEPC and PPDK were migrating as a super-complex. This observation led us to hypothesize that these proteins were cooperating in the form of a metabolon. To confirm this, the band was excised from the native gel and incubated in a solution containing citrate, AMP and PP_i. After 30 min, the reaction mixture was subjected to HPLC analysis for the presence of reaction products. Indeed, the concentration of substrates was lowered and there was an appearance of distinct peaks characteristic of PEP, pyruvate, ATP and oxaloacetate (Fig. 2C). The possibility of a physical link between the three enzymes prompted us to immunoprecipitate PEPC to analyze the presence of attached proteins. Although antibodies against bacterial CL are not commercially available, PPDK was readily identified via Western blot. PEPC was also detected when PPDK was pulled down, while neither enzyme was detected in the control cells. (Fig. 2D).

The assembly of metabolic complexes referred to as metabolons is often transient, and brought about by distinct post-translational modifications [31,32]. This allows them to form rapidly and come apart when the needs of the cell are met. Incubation of the soluble fraction of the organism with alkaline phosphatase for 15 min prior to BN-PAGE was applied to separate the three enzymes. Following this treatment, CL and PEPC activity bands were identified at their respective molecular mass lower in the gel in comparison to when they migrated as a metabolon (Fig. 3A). PPDK activity was noticeably absent after dephosphorylation, thus indicating the importance of this modification to the function of the enzyme. To demonstrate this finding, the band for PPDK was excised and run through a SDS-PAGE gel. Both antibodies against PPDK and antibodies against phosphorylated amino acid residues generated a yellow signal at 60 kDA, the reported molecular mass of this enzyme (Fig. 3B). PPDK and phosphorylated proteins could be detected separately in the green (800 nm) and red (680 nm) channels, respectively (Fig. 3C).

Activity assays were applied to measure the activity of phosphotransfer enzymes in the cell, as these allow for the storage of high-energy phosphate [5]. Acetate kinase, which phosphorylates acetate and thus facilitates the production of acetyl-CoA, was found to be up-regulated in the stressed cells (Fig. 4A). NDPK allows the transfer of high energy phosphate between nucleosides and also displayed higher activity than the control cultures (Fig. 4A). PPase, which catalyzes the breakdown of PP_i into two phosphate ions, was analyzed in order to understand why PP_i levels were elevated in the NO-treated cultures. Indeed, this enzyme had diminished activity in the stressed cells (Fig. 4A). Adenylate kinase, which takes two ADP molecules and generates ATP and AMP, also had higher activity in the RNS-treated cultures (Fig. 4A). To ascertain the nature of the enzyme, activity bands are routinely excised and incubated in their respective substrates. The band indicative of AK was cut out of the gel from the control (Fig. 4B, i) and SNP-treated (Fig. 4B, ii) lanes and incubated in 1 mM ADP for 45 min. As seen in the chromatograms, ADP was consumed quicker in the SNP-treated cells, and the appearance of ATP and AMP was more pronounced, indicating an increased activity of the enzyme.

4. Discussion

The data presented here describe a novel metabolic pathway aimed at ATP production (Fig. 5). Nitrosative stress brings about the assembly of CL, PEPC and PPDK, three enzymes which allow the production of ATP when the ETC of *P. fluorescens* is defective. It is a common perception that enzymes diffuse freely in biological systems, catalyzing their respective reactions when metabolites interact with them via passive diffusion. However, the formation of enzyme or protein aggregates is a more likely event as these enable metabolic networks to be more proficient. The benefits of such an arrangement are numerous. The close proximity between sequential enzymes allows the product of one reaction to be channeled to the next without equilibrating with the bulk cellular fluid. Such an event also assures a greater degree of specificity, allowing metabolites that are acted upon by a number of proteins to be funneled towards the desired end product. Indeed, these protein-protein interactions may allow certain reactions to transpire *in vivo* that would not occur if the enzyme was unaccompanied [33–35]. Although these interactions are usually fragile and difficult to study, techniques such as BN-PAGE afford a potent tool to decipher these metabolons [35,36].

It has long been known that the presence of heme groups and iron-sulfur clusters within the electron transport chain render these complexes susceptible to oxidative and nitrosative stress. Indeed, this vulnerability underlies the success of white blood cells and their ability to subdue invading pathogens, as the formation of noxious radicals by NADPH oxidase and inducible nitric oxide synthase are key tools in combatting infectious microbes [37,38]. Here, we show that the presence of SNP or DEANO in the growth medium has a detrimental effect on ATP-formation via oxidative phosphorylation, as visualized by in-gel enzyme activity assays and HPLC. Previous studies have reported

that, under nitrosative stress, the microbe survives by rerouting citrate away from the tricarboxylic acid cycle using CL in an effort to generate ATP anaerobically [11]. This metabolic shift is to be expected, since the first three enzymes of the TCA cycle are sensitive to free radicals, as evidenced by their reduced activity [11,39–41]. We postulated that, on the basis of their migration together in the BN-PAGE unit, CL, PEPC and PPDK were acting in tandem, thus presenting a means by which ATP could be generated efficiently for the survival of the organism [11]. Incubation of the band from the in-gel activity assay with the proper substrates and co-immunoprecipitation were applied to confirm this hypothesis. Initial attempts to understand how this supercomplex was assembled *in vivo* included Western blots to analyze the presence of acetylated or nitrosylated residues on the proteins, moieties that are expected given the environmental conditions of the cell. However, these modifications were not found (data not shown). Incubation of the soluble cell free extract with alkaline phosphatase prior to performing BN-PAGE was effective in separating the metabolon, indicating that a phosphorylation event is responsible for bringing these proteins in close contact. Indeed, this post-translational modification also appears to be responsible for the increase in PPDK activity. Although we are the first to report on this unique multiprotein complex designed to generate ATP, others have described metabolons involving glycolytic and TCA cycle enzymes, thus lending further support to the notion that metabolic enzymes rarely function unaccompanied in biological systems [35,42,43]. A similar association involving PEPC and PPDK is evident in the presence of such carbon source as glucose and glutamate (personal observation).

It is of interest to note that, whereas CL and PEPC mediate the conversion of citrate into the high-energy intermediate PEP, it is PPDK which converts this moiety into pyruvate and ATP, a role normally fulfilled by PK. While the latter utilizes ADP as a cofactor for this reaction, PPDK employs AMP and PP_i. The substitution of PPDK for PK is immensely beneficial to the organism, especially in conditions where oxidative phosphorylation is rendered inadequate. This dikinase is more commonly found in plants and anaerobic parasites such as *Trypanosoma spp.* and *Entamoeba spp.*, where it presents itself as a novel therapeutic target due to the lack of PPDK analogues in mammalian systems [44,45]. Energy efficiency may be an important consideration behind the preference for PPDK, as this enzyme can utilize PP_i instead of ADP. The participation of PPDK, coupled to the activity of adenylate kinase, permits the production of two ATP per molecule of PEP, while traditional glycolysis can only generate one [46]. Under energy-limiting conditions, such as those invoked by the inactivation of the electron transport chain, this adaptation becomes vital.

Indeed, both PPDK and AK display increased activity in our system when exposed to NO stress. For this stratagem to remain sustainable, the maintenance of a PP_i pool is required to drive this reaction forward. Pyrophosphate is formed as a byproduct in a plethora of synthetic reactions, such as those involved in the synthesis of macromolecules like DNA and proteins [47]. However, the energy stored in the anhydride bond of PP_i is not utilized as the ubiquitous inorganic pyrophosphatase (PPase) immediately hydrolyses this compound to P_i [48]. Here, the down-regulation of PPase activity would certainly allow the PP_i concentration in the cell to remain elevated in an effort to propel PPDK activity. It is not unlikely that the increase in intracellular PP_i inactivates PK, as the former is known to be an allosteric inhibitor of this enzyme [47]. The increased activities of phosphotransfer enzymes such as AK and NDPK, which allow the storage and distribution of high-energy phosphate, would also drive the continued activity of PPDK while fulfilling the need for nucleotides in cellular division. Indeed, the existence of phosphowires allows for the proper functioning of complex V. In this instance, ADP is converted into ATP and the energy shuttled via AK, NDPK as well as creatine kinase [5].

In conclusion, this report reveals how an intricate arrangement involving CL, PEPC and PPDK allows for the effective generation of ATP when oxidative phosphorylation is compromised by nitrosative stress. This metabolic complex that appears to hinge on the alkaline phosphatase-sensitive PPDK mediates the conversion of citrate into pyruvate and ATP with the participation of AMP and PP_i. A phosphotransfer system propelled by ACK, NDPK and AK generates various high-energy compounds with the concomitant formation of AMP, a key ingredient that fuels the metabolon. The pivotal role metabolism and this multi-enzyme complex play in the survival of this microbe provides important therapeutic cues against RNS-resistant bacteria.

Acknowledgments

This work was supported by Laurentian University. Christopher Auger is a recipient of the NSERC post-graduate scholarship at the doctoral level.

References

[1] C. von Ballmoos, A. Wiedenmann, P. Dimroth, Essentials for ATP synthesis by F1F0 ATP synthases, Annu. Rev. Biochem. 78 (2009) 649–672.
[2] P.P. Dzeja, P. Bast, D. Pucar, B. Wieringa, A. Terzic, Defective metabolic signaling in adenylate kinase AK1 gene knock-out hearts compromises post-ischemic coronary reflow, J. Biol. Chem. 282 (2007) 31366–31372.
[3] M. Bonora, S. Patergnani, A. Rimessi, E. De Marchi, J.M. Suski, A. Bononi, C. Giorgi, S. Marchi, S. Missiroli, F. Poletti, M.R. Wieckowski, P. Pinton, ATP synthesis and storage, Purinergic Signal 8 (2012) 343–357.
[4] A.J. Carrasco, P.P. Dzeja, A.E. Alekseev, D. Pucar, L.V. Zingman, M.R. Abraham, D. Hodgson, M. Bienengraeber, M. Puceat, E. Janssen, B. Wieringa, A. Terzic, Adenylate kinase phosphotransfer communicates cellular energetic signals to ATP-sensitive potassium channels, Proc. Natl. Acad. Sci. U. S. A. 98 (2001) 7623–7628.
[5] P.P. Dzeja, A. Terzic, Phosphotransfer networks and cellular energetics, J. Exp. Biol. 206 (2003) 2039–2047.
[6] J. Lemire, R. Mailloux, C. Auger, D. Whalen, V.D. Appanna, *Pseudomonas fluorescens* orchestrates a fine metabolic-balancing act to counter aluminium toxicity, Environ. Microbiol. 12 (2010) 1384–1390.
[7] V. Coustou, S. Besteiro, M. Biran, P. Diolez, V. Bouchaud, P. Voisin, P.A. Michels, P. Canioni, T. Baltz, F. Bringaud, ATP generation in the *Trypanosoma brucei* procyclic form: cytosolic substrate level is essential, but not oxidative phosphorylation, J. Biol. Chem. 278 (2003) 49625–49635.
[8] F. Bringaud, D. Baltz, T. Baltz, Functional and molecular characterization of a glycosomal PPi-dependent enzyme in trypanosomatids: pyruvate, phosphate dikinase, Proc. Natl. Acad. Sci. U. S. A. 95 (1998) 7963–7968.
[9] A. Bignucolo, V.P. Appanna, S.C. Thomas, C. Auger, S. Han, A. Omri, V.D. Appanna, Hydrogen peroxide stress provokes a metabolic reprogramming in *Pseudomonas fluorescens*: enhanced production of pyruvate, J. Biotechnol. 167 (2013) 309–315.
[10] S.B. Wang, C.I. Murray, H.S. Chung, J.E. Van Eyk, Redox regulation of mitochondrial ATP synthase, Trends Cardiovasc. Med. 23 (2013) 14–18.
[11] C. Auger, J. Lemire, D. Cecchini, A. Bignucolo, V.D. Appanna, The metabolic reprogramming evoked by nitrosative stress triggers the anaerobic utilization of citrate in *Pseudomonas fluorescens*, PLoS One 6 (2011) e28469.
[12] K. Poole, Stress responses as determinants of antimicrobial resistance in Gram-negative bacteria, Trends Microbiol. 20 (2012) 227–234.
[13] J.R. Laver, T.M. Stevanin, S.L. Messenger, A.D. Lunn, M.E. Lee, J.W. Moir, R.K. Poole, R.C. Read, Bacterial nitric oxide detoxification prevents host cell S-nitrosothiol formation: a novel mechanism of bacterial pathogenesis, FASEB J. 24 (2010) 286–295.
[14] M. Shepherd, V. Barynin, C. Lu, P.V. Bernhardt, G. Wu, S.R. Yeh, T. Egawa, S.E. Sedelnikova, D.W. Rice, J.L. Wilson, R.K. Poole, The single-domain globin from the pathogenic bacterium *Campylobacter jejuni*: novel D-helix conformation, proximal hydrogen bonding that influences ligand binding, and peroxidase-like redox properties, J. Biol. Chem. 285 (2010) 12747–12754.
[15] A. Chapalain, G. Rossignol, O. Lesouhaitier, A. Merieau, C. Gruffaz, J. Guerillon, J.M. Meyer, N. Orange, M.G. Feuilloley, Comparative study of 7 fluorescent pseudomonad clinical isolates, Can. J. Microbiol. 54 (2008) 19–27.
[16] S. Anderson, V.D. Appanna, J. Huang, T. Viswanatha, A novel role for calcite in calcium homeostasis, FEBS Lett. 308 (1992) 94–96.
[17] R. Singh, J. Lemire, R.J. Mailloux, D. Chenier, R. Hamel, V.D. Appanna, An ATP and oxalate generating variant tricarboxylic acid cycle counters aluminum toxicity in *Pseudomonas fluorescens*, PLoS One 4 (2009) e7344.
[18] T.J. Bourret, J.A. Boylan, K.A. Lawrence, F.C. Gherardini, Nitrosative damage to free and zinc-bound cysteine thiols underlies nitric oxide toxicity in wild-type *Borrelia burgdorferi*, Mol. Microbiol. 81 (2011) 259–273.
[19] A. Rogstam, J.T. Larsson, P. Kjelgaard, C. von Wachenfeldt, Mechanisms of adaptation to nitrosative stress in *Bacillus subtilis*, J. Bacteriol. 189 (2007) 3063–3071.
[20] P. Kumar, R.K. Tewari, P.N. Sharma, Sodium nitroprusside-mediated alleviation of iron deficiency and modulation of antioxidant responses in maize plants, AoB Plants 2010 (2010) plq002.
[21] M.M. Bradford, A rapid and sensitive method for the quantitation of microgram quantities of protein utilizing the principle of protein-dye binding, Anal. Biochem. 72 (1976) 248–254.
[22] H. Schagger, G. von Jagow, Blue native electrophoresis for isolation of membrane protein complexes in enzymatically active form, Anal. Biochem. 199 (1991) 223–231.

[23] R.J. Mailloux, R. Singh, G. Brewer, C. Auger, J. Lemire, V.D. Appanna, Alpha-ketoglutarate dehydrogenase and glutamate dehydrogenase work in tandem to modulate the antioxidant alpha-ketoglutarate during oxidative stress in *Pseudomonas fluorescens*, J. Bacteriol. 191 (2009) 3804–3810.
[24] J. Lemire, Y. Milandu, C. Auger, A. Bignucolo, V.P. Appanna, V.D. Appanna, Histidine is a source of the antioxidant, alpha-ketoglutarate, in *Pseudomonas fluorescens* challenged by oxidative stress, FEMS Microbiol. Lett. 309 (2010) 170–177.
[25] C. Auger, V. Appanna, Z. Castonguay, S. Han, V.D. Appanna, A facile electrophoretic technique to monitor phosphoenolpyruvate-dependent kinases, Electrophoresis 33 (2012) 1095–1101.
[26] R.J. Mailloux, R. Darwich, J. Lemire, V. Appanna, The monitoring of nucleotide diphosphate kinase activity by blue native polyacrylamide gel electrophoresis, Electrophoresis 29 (2008) 1484–1489.
[27] E.E. Hernandez-Domiguez, L.G. Valencia-Turcotte, R. Rodriguez-Sotres, Changes in expression of soluble inorganic pyrophosphatases of *Phaseolus vulgaris* under phosphate starvation, Plant Sci. 187 (2012) 39–48.
[28] U.K. Laemmli, Cleavage of structural proteins during the assembly of the head of bacteriophage T4, Nature 227 (1970) 680–685.
[29] R. Van Coster, J. Smet, E. George, L. De Meirleir, S. Seneca, J. Van Hove, G. Sebire, H. Verhelst, J. De Bleecker, B. Van Vlem, P. Verloo, J. Leroy, Blue native polyacrylamide gel electrophoresis: a powerful tool in diagnosis of oxidative phosphorylation defects, Pediatr. Res. 50 (2001) 658–665.
[30] G.J. Fiala, W.W. Schamel, B. Blumenthal, Blue native polyacrylamide gel electrophoresis (BN-PAGE) for analysis of multiprotein complexes from cellular lysates, J. Vis. Exp. 48 (2011) 2164.
[31] M. Bartholomae, F.M. Meyer, F.M. Commichau, A. Burkovski, W. Hillen, G. Seidel, Complex formation between malate dehydrogenase and isocitrate dehydrogenase from *Bacillus subtilis* is regulated by tricarboxylic acid cycle metabolites, FEBS J. (2013), http://dx.doi.org/10.1111/febs.12679.
[32] D. Araiza-Olivera, N. Chiquete-Felix, M. Rosas-Lemus, J.G. Sampedro, A. Pena, A. Mujica, S. Uribe-Carvajal, A glycolytic metabolon in *Saccharomyces cerevisiae* is stabilized by F-actin, FEBS J. 280 (2013) 3887–3905.
[33] D. Sowah, J.R. Casey, An intramolecular transport metabolon: fusion of carbonic anhydrase II to the COOH terminus of the Cl(-)/HCO(3)(-)exchanger, AE1, Am. J. Physiol. Cell Physiol. 301 (2011) C336–C346.
[34] H.L. McMurtrie, H.J. Cleary, B.V. Alvarez, F.B. Loiselle, D. Sterling, P.E. Morgan, D.E. Johnson, J.R. Casey, The bicarbonate transport metabolon, J. Enzyme Inhib. Med. Chem. 19 (2004) 231–236.
[35] B.S. Winkel, Metabolic channeling in plants, Annu. Rev. Plant Biol. 55 (2004) 85–107.
[36] M.P. Williamson, M.J. Sutcliffe, Protein–protein interactions, Biochem. Soc. Trans. 38 (2010) 875–878.
[37] S. Kroller-Schon, S. Steven, S. Kossmann, A. Scholz, S. Daub, M. Oelze, N. Xia, M. Hausding, Y. Mikhed, E. Zinssius, M. Mader, P. Stamm, N. Treiber, K. Scharffetter-Kochanek, H. Li, E. Schulz, P. Wenzel, T. Munzel, A. Daiber, Molecular mechanisms of the crosstalk between mitochondria and NADPH oxidase through reactive oxygen species-studies in white blood cells and in animal models, Antioxid. Redox Signal. 20 (2014) 247–266.
[38] M.N. Alvarez, G. Peluffo, L. Piacenza, R. Radi, Intraphagosomal peroxynitrite as a macrophage-derived cytotoxin against internalized *Trypanosoma cruzi*: consequences for oxidative killing and role of microbial peroxiredoxins in infectivity, J. Biol. Chem. 286 (2011) 6627–6640.
[39] E.S. Yang, C. Richter, J.S. Chun, T.L. Huh, S.S. Kang, J.W. Park, Inactivation of NADP(+)-dependent isocitrate dehydrogenase by nitric oxide, Free Radic. Biol. Med. 33 (2002) 927–937.
[40] K.J. Gupta, J.K. Shah, Y. Brotman, K. Jahnke, L. Willmitzer, W.M. Kaiser, H. Bauwe, A.U. Igamberdiev, Inhibition of aconitase by nitric oxide leads to induction of the alternative oxidase and to a shift of metabolism towards biosynthesis of amino acids, J. Exp. Bot. 63 (2012) 1773–1784.
[41] A.R. Richardson, E.C. Payne, N. Younger, J.E. Karlinsey, V.C. Thomas, L.A. Becker, W.W. Navarre, M.E. Castor, S.J. Libby, F.C. Fang, Multiple targets of nitric oxide in the tricarboxylic acid cycle of *Salmonella enterica serovar typhimurium*, Cell Host Microbe 10 (2011) 33–43.
[42] R.A. Reithmeier, A membrane metabolon linking carbonic anhydrase with chloride/bicarbonate anion exchangers, Blood Cells Mol. Dis. 27 (2001) 85–89.
[43] P. Dhar-Chowdhury, M.D. Harrell, S.Y. Han, D. Jankowska, L. Parachuru, A. Morrissey, S. Srivastava, W. Liu, B. Malester, H. Yoshida, W.A. Coetzee, The glycolytic enzymes, glyceraldehyde-3-phosphate dehydrogenase, triose-phosphate isomerase, and pyruvate kinase are components of the K(ATP) channel macromolecular complex and regulate its function, J. Biol. Chem. 280 (2005) 38464–38470.
[44] E. Saavedra, R. Encalada, E. Pineda, R. Jasso-Chavez, R. Moreno-Sanchez, Glycolysis in *Entamoeba histolytica*. Biochemical characterization of recombinant glycolytic enzymes and flux control analysis, FEBS J. 272 (2005) 1767–1783.
[45] C.H. Slamovits, P.J. Keeling, Pyruvate-phosphate dikinase of oxymonads and parabasalia and the evolution of pyrophosphate-dependent glycolysis in anaerobic eukaryotes, Eukaryot. Cell 5 (2006) 148–154.
[46] C.J. Chastain, C.J. Failing, L. Manandhar, M.A. Zimmerman, M.M. Lakner, T.H. Nguyen, Functional evolution of C(4) pyruvate, orthophosphate dikinase, J. Exp. Bot. 62 (2011) 3083–3091.
[47] A.A. Bielen, K. Willquist, J. Engman, J. van der Oost, E.W. van Niel, S.W. Kengen, Pyrophosphate as a central energy carrier in the hydrogen-producing extremely thermophilic *Caldicellulosiruptor saccharolyticus*, FEMS Microbiol. Lett. 307 (2010) 48–54.
[48] D. Deamer, A.L. Weber, Bioenergetics and life's origins, Cold Spring Harb. Perspect. Biol. 2 (2010) a004929.